

A new optical sensor for real time in-situ endpoint monitoring during dry etching of III-V Ternary Multi Stack Layers

Susan Maher*^a, Ramdane Benferhat^b, Jewon Lee^c, Dave Johnson^c, John F. Donahue^c, Jay N. Sasserath^c,

^aThin Film Group, Instruments SA, Inc./ Horiba Group, 3880 Park Ave, Edison, NJ 08820

^bThin Film Group, Instruments S.A./ Horiba Group, 7 rue d'Egly, 91290 Arpajon, France

^cPlasma-Therm, Inc. 10050 16th St. Petersburg, FL 33716

Abstract

There has been a great demand for improved end point detection techniques for advanced etching of III-V ternary multi stack layers. Current etch rate and end point monitoring techniques are based on three methods. The first is to use timed or a blind etch as it is known, this offers no monitoring of the etch process. The second is to use optical emission spectroscopy (OES) which is a secondary measurement of the process and requires a large open area, fast etch rate, and a detectable emission line from the etch products. The third is laser interferometry, a primary measurement, based on light interference of reflected beams from several layers in the stack.

Up to now the use of commercially available interferometric techniques has not permitted the measurement of etch rates and end point the etch processes due to the absorption of the wavelengths of light available in current process control systems.

A new in-situ end point system utilizing a 905nm laser interferometer will be described that allows the ability to follow dry etching of III-V ternary multi stack layers. End point detection techniques on various $\text{Al}_x\text{Ga}_{1-x}\text{As}$ with different compositions (i.e. $x=0.3-0.92$) and different types (n- or p- AlGaAs) are examined.

Keywords: III-V Materials, Etch Rate Measurement, Laser interferometry, End Point Control, Process Control Instrumentation, Wafer Fabrication Equipment

1. Introduction

There is a great demand for improved endpoint detection and process control systems for advanced etching of III-V multistack layers such as $\text{Al}_x\text{Ga}_{1-x}\text{As}$ on GaAs layers. A variety of techniques have been used including optical emission spectroscopy (OES)⁽¹⁻³⁾, reflectometry⁽⁶⁻¹¹⁾.

Current monitoring approaches have focused on two methods. The first is optical emission spectroscopy, which requires a relatively large wafer, fast etch rate and a detectable emission line from etch byproducts. This method is not a primary measurement of the process but looks at secondary evidence in the etched product emission spectrum. A second method is based on light interference and refractive index of materials. An Infrared laser source has been employed previously as an endpoint technique for III-V semiconductor etching because of its possible advantages over the OES method in terms of sample size and accuracy of interpretation.⁽¹⁻³⁾ The use of a conventional 670 nm laser source has difficulty in producing distinguishable interference patterns with either $\text{Al}_x\text{Ga}_{1-x}\text{As}$ (where $x \sim 0.3$, transmitting wavelength is 790 nm) or GaAs (where transmitting wavelength is 918 nm) layers due to absorption in the materials. The light from a 670 nm laser is strongly absorbed in GaAs and $\text{Al}_x\text{Ga}_{1-x}\text{As}$ materials and heterostructure interferometry is limited to optically thin ($< 5000 \text{ \AA}$) layers.

For etch rate monitoring of thicker layers, either specific diffraction test patterns or longer wavelength must be employed. For example, light from a 905 nm wavelength infrared laser exhibits some interference with $\text{Al}_x\text{Ga}_{1-x}\text{As}$, and no interference with GaAs due to absorption, which will produce a noticeable difference of signal patterns for etching of the two materials. The transmission wavelengths of GaAs and $\text{Al}_{0.27}\text{Ga}_{0.73}\text{As}$ are 918 and 790 nm, respectively, and 905 nm is between the two wavelengths. In this case, we can utilize a 905 nm wavelength laser as a new source for in-situ end point detection for $\text{Al}_x\text{Ga}_{1-x}\text{As}/\text{GaAs}$ etching.

2. GENERAL FORMALISM OF INTERFEROMETRY

Reflection of light at smooth interface between two media with different refractive indices are described by the Fresnel equations which can be derived using the boundary conditions for the electromagnetic field. If we define as n_a the complex refractive index of the ambient and n_s as the complex refractive index of a bare substrate, the complex reflection coefficient at normal incidence of a continuous tangential electromagnetic field is then described by relation [2.1] :

$$r_{a,s} = (n_a - n_s) / (n_a + n_s) \quad [2.1] \quad \text{with} \quad n_{a,s} = n_{a,s} - j k_{a,s}$$

$k_{a,s}$ being the extinction coefficient and $n_{a,s}$ the refractive index for respectively the ambient and the substrate.

If the system above is extended to a system including a homogenous and isotropic film of thickness d_f and optical properties $n_f = n_f - j k_f$ and by taking into account the multiple reflection inside the film , one can derive the complex reflection coefficients of an electromagnetic field :

$$r = (r_{a,f} + r_{f,s} e^{-j2\beta}) / (1 + r_{a,f} r_{f,s} e^{-j2\beta}) \quad [2.2]$$

Where $\beta = 2 \pi n_f d_f / \lambda$, $r_{a,f}$ and $r_{f,s}$ are respectively the complex reflection coefficient of the light at the interface ambient-film and film-substrate. If we define α as the absorption coefficient of the film and L_p the penetration depth of light :

$$\alpha = 4 \pi k_f / \lambda$$

$$L_p = 1/\alpha$$

The complex reflection coefficient of light which can be derived from [2.2] :

$$r = (r_{a,f} + r_{f,s} e^{-j2\delta} e^{-d_f / L_p}) / (1 + r_{a,f} r_{f,s} e^{-j2\delta} e^{-d_f / L_p}) \quad \text{with} \quad \delta = 2 \pi n_f d_f / \lambda$$

If $d_f \gg L_p$, the probing light is completely absorbed by the layer and $r \sim r_{a,f}$. The interference effect will disappear. For more convenience, we can define the penetration depth as the maximum thickness which can be probed.

Reference	L_p at 670 nm	L_p at 905 nm
GaAs	0.315 μm	72 μm
$\text{Al}_x\text{Ga}_{(1-x)}\text{As}$ $x = 0.27$	0.6 μm	$\gg 100 \mu\text{m}$
$\text{Al}_x\text{Ga}_{(1-x)}\text{As}$ $x = 0.5$	53 μm	$\gg 100 \mu\text{m}$
$\text{Al}_x\text{Ga}_{(1-x)}\text{As}$ $x = 0.92$	$\gg 100 \mu\text{m}$	$\gg 100 \mu\text{m}$

Table 1 shows the penetration depth of light at two wavelengths of our GaAs and $\text{Al}_x\text{Ga}_{1-x}\text{As}$ (i.e. $x = 0.3 \sim 0.92$) samples.

3. SYSTEM DESCRIPTION

The new infrared interferometric camera is manufactured by the Thin Film Group of Instruments SA / Horiba. The system is based on the use of a 905nm laser diode as a probing beam for making interferometric measurements of III-V materials. The system is composed of the 905nm laser diode, a silicon photodiode for signal acquisition, a CCD chip for producing a video image of the wafer surface, an illumination source for the CCD, and a set of objective lenses for focusing the illumination source and the laser onto the wafer surface and then collecting the reflected light from the wafer.

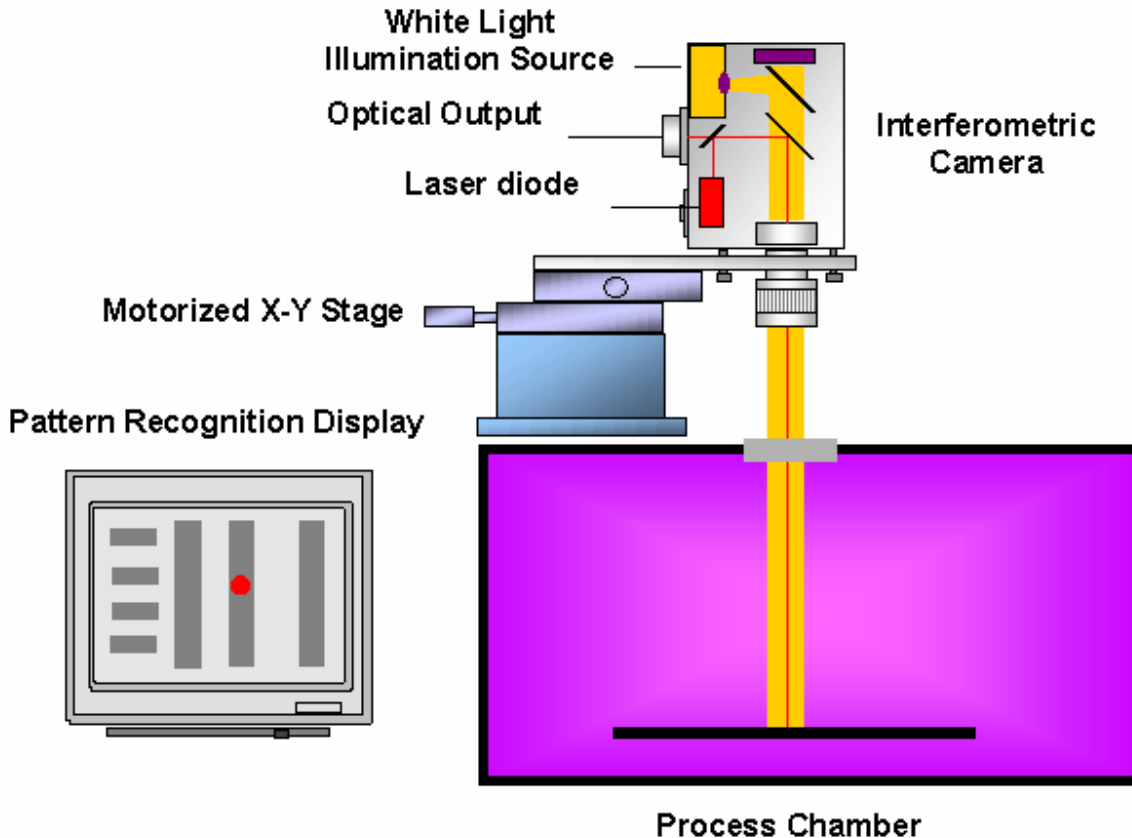


Fig 1. Optical diagram of IR interferometric Camera

The light emitted by the laser diode is focused by a set of objective lenses and is focused onto the wafer surface through the chamber window. The reflected beam is then collected back through the same objective lens set and follows the exact path back through the system until it impacts a beam splitter where a portion of the light passes through and is detected by a silicon photodiode.

In the back of the camera there is a CCD chip and halogen light source for illuminating the wafer for the video image. The CCD chip optical axis is in a direct line to the wafer surface. A white light illumination source is projected through a focusing lens and turning mirror in a manner that allows projection of the illumination light onto the wafer surface and collection of the image back to the CCD chip.

The camera is mounted on either a manual or motorized X-Y translation stage. The manual translation stage allows positioning of the beam by using the video image of the wafer surface as a reference. The manual X-Y stage has 16mm of travel in each direction.

The CCD sensitivity is good to just above 1 μ m thus allowing a visual image of the laser spot on the wafer surface. The system can also use a motorized X-Y translation stage with 25mm of travel in each direction. The motorized stage is

typically used with a pattern recognition software program and the video image to allow automatic positioning of the laser beam on user defined locations.

The system was mounted on A Plasma-Therm load-locked SLR 770 Inductively Coupled Plasma (ICP) etcher utilizing a 2MHz rf frequency for etching the materials. The process chemistry employed 20 standard cubic centimeter per minute (sccm) BCl_3 , 5mTorr chamber pressure, 100W rf chuck power and 800 W ICP source power. Etch depths were measured with Tencor profilometry after etching. 0.2-2.0 μm thick $\text{Al}_x\text{Ga}_{1-x}\text{As}$ ($x=0.3-0.92$) layers were grown on bulk GaAs wafers and were used in the evaluation of the system.

4. RESULTS AND DISCUSSION

In Fig 2 Are displayed in-situ monitoring results during etching of $\text{Al}_{0.28}\text{Ga}_{0.82}\text{As}/\text{GaAs}$ heterostructure with a conventional 670 nm laser module. Due to the small penetration depth of light in the layer, no distinguishable interference pattern was obtained. In all case, all of 670 nm wavelength laser beam was absorbed in the materials.

Relative Intensity

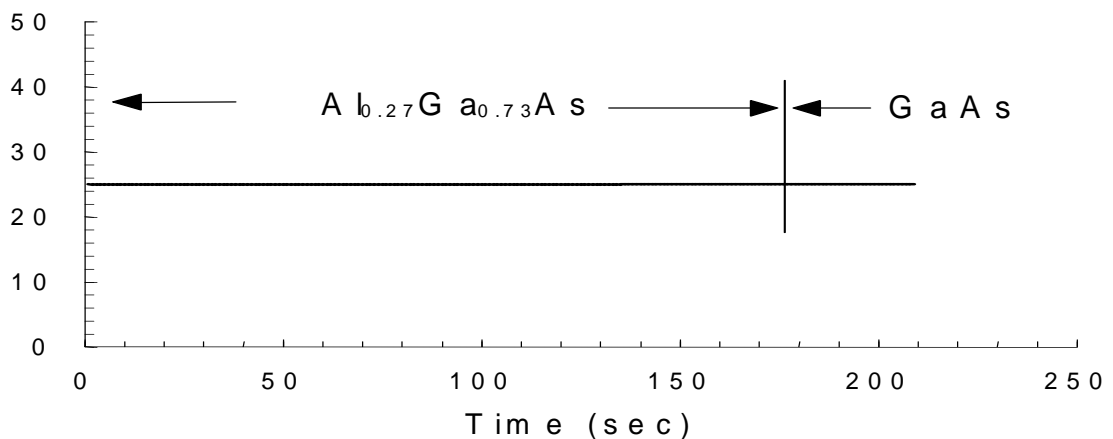


Fig 2. Interferometric trace of $\text{Al}_{0.27}\text{Ga}_{0.73}\text{As}/\text{GaAs}$ etch using 670 nm laser based interferometric camera

Figure 3 depicts monitored results with a 905 nm laser for etching of a heterostructure. Note that there was a clear interference pattern for AlGaAs etching and it disappeared for GaAs etching.

High Al composition increased the magnitude of interference intensity for AlGaAs etching (Figure 4). Note also that the interference wavelength of the laser with both a 50 % and 92 % Al composition in AlGaAs during etching was significant, however the difference was minimal for etching with compositions containing 28 % and 50 % Al in AlGaAs (refer Figure 3 and Figure 4 (top)).

Monitoring results of n+ and p+ type AlGaAs etching are shown in Figure 6 and 7 respectively. Total etch depths of p+ AlGaAs/GaAs, n+ AlGaAs/GaAs were measured as 2000 Å, 5936 Å, respectively, after etching. Use of the 905 nm laser produced excellent interference patterns with both n and p-type AlGaAs etching even for relatively thin layers (p-type case).

Relative Intensity

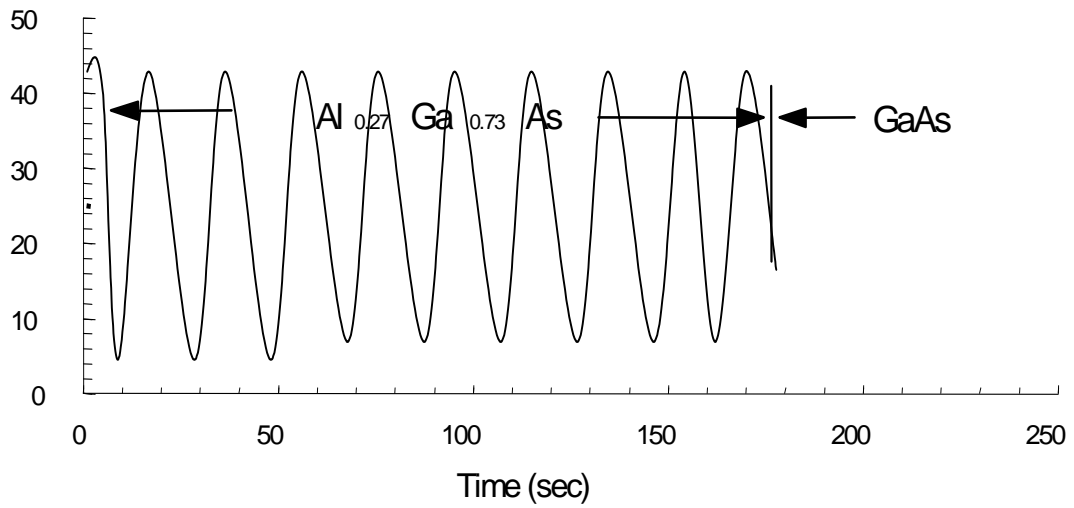


Fig 3. Interferometric trace of $Al_{0.27}Ga_{0.73}As/GaAs$ etch using 905 nm laser based interferometric camera

Relative Intensity

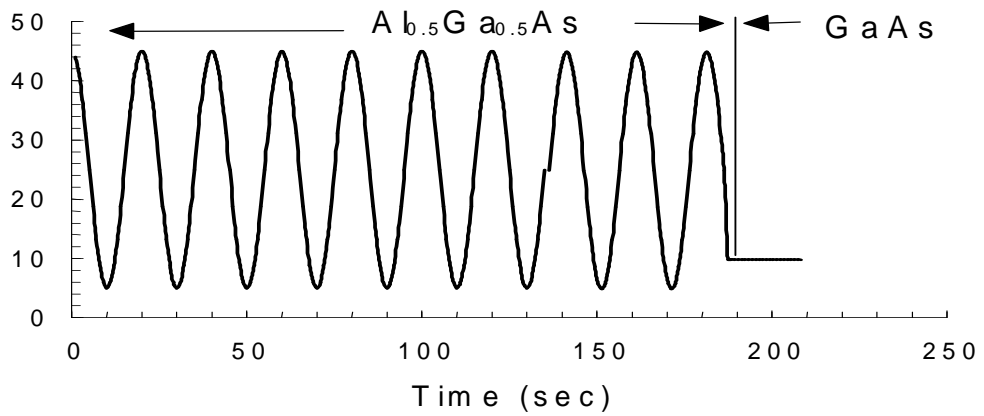


Fig 4. Interferometric trace of $Al_{0.5}Ga_{0.5}As/GaAs$ etch using 905 nm laser based interferometric camera

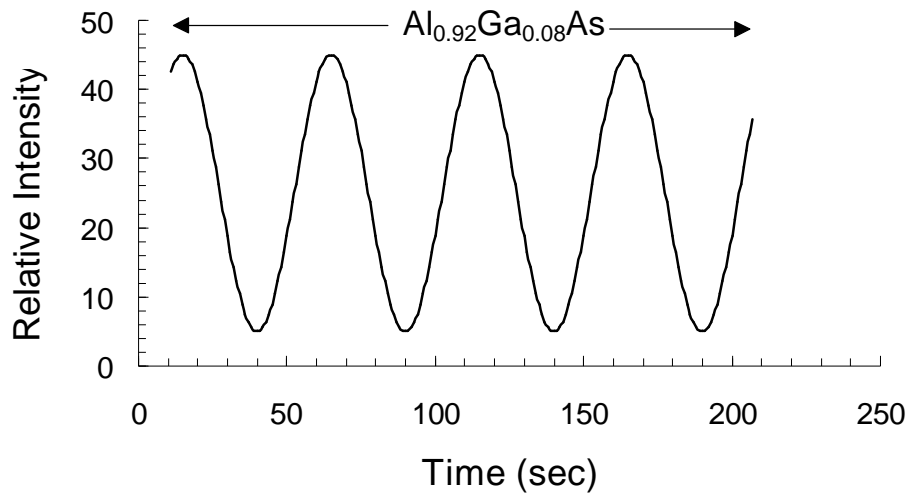


Fig 5. Interferometric trace of $\text{Al}_{0.92}\text{Ga}_{0.08}\text{As}/\text{GaAs}$ etch using 905 nm laser based interferometric camera

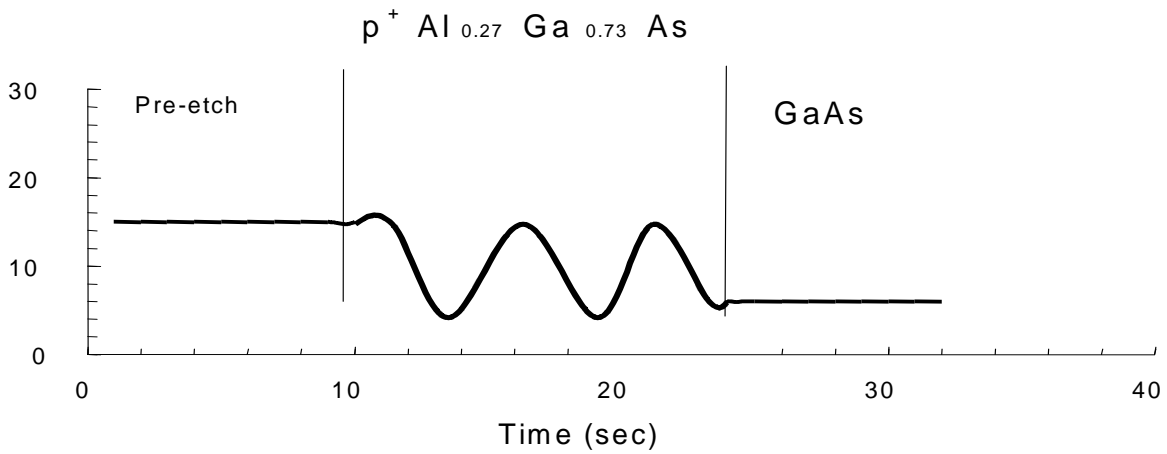


Fig 6. Interferometric trace of $\text{p}^+ \text{Al}_{0.27}\text{Ga}_{0.73}\text{As}/\text{GaAs}$ etch using 905 nm laser based interferometric camera

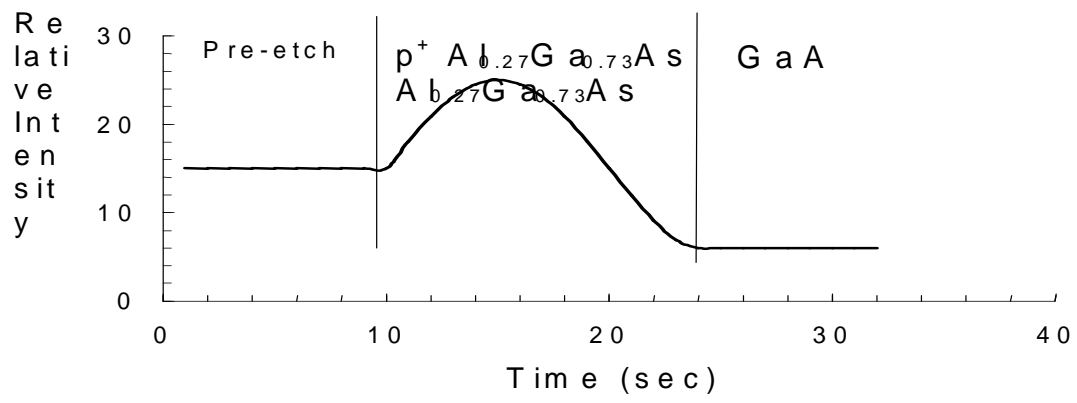


Fig 7. Interferometric trace of n⁺Al_{0.27}Ga_{0.73}As /GaAs etch using 905 nm laser based interferometric camera

SUMMARY AND CONCLUSION

A new Endpoint camera sensor for dry etching of $\text{Al}_x\text{Ga}_{1-x}\text{As}/\text{GaAs}$ layers has been described. As compared to other interferometric techniques, this new sensor camera takes advantages of the use of a 905 nm laser diode combined with imaging capabilities. A successful demonstration of its capability as an in-situ end point detector is described. Combined with the well known ISA – Jobin Yvon – Sofie multisensor, the MULTISEM 550 platform, we have today a complete solution for a total control of etch processes in the field of III-V based devices.

References

1. P. Collot, T. Diallo and J. Canteloup, *J. Vac. Sci. Technol. B* **9** 2897 (1991).
2. S. J. Pearton, F. Ren, C. R. Abernathy and C. Constantine, *Mat. Sci. Eng. B* **23** 36 (1994).
3. R. Collot, T. Diallo and J. Canteloup, *Proc. Electrochem. Soc.* **91-13** 114 (1991).
4. K. L. Seaward, N. J. Moll, D. J. Coulman and W. F. Stickle, *J. Appl. Phys.* **61** 2358 (1997).
5. I. Hase, K. Taira, H. Kawai, K. Kaneto and N. Watanabe, *J. Vac. Sci. Technol. B* **7** 618 (1989).
6. T. P. Pearsall, *Proc. Electrochem. Soc.* **94-18** 286 (1994).
7. S. Thomas III, H. H. Chen, C. K. Hanish, J. W. Grizzle and S. W. Pang, *J. Vac. Sci. Technol. B* **14** 253 (1996).
8. G. Franz, C. Hoyler and J. Kaindl, *J. Vac. Sci. Technol. B* **14** 126 (1996).
9. J. F. Klern, W. G. Breiland, L. J. Fritz, T. J. Drcmmand and S. R. Lee, *J. Vac. Sci. Technol. B* **16** 1498 (1998).
10. T. R. Hayes, in *InP and Related Compounds*, ed. A. Katz (Artech House, Dedham MA 1989).
11. A. Mitchell, R. A. Gottscho, S. J. Pearton and G. R. Scheller, *Appl. Phys. Lett.* **56** 821 (1990).
12. M. Takai, H. Nakai, J. Tsuchimoto, K. Gamo and S. Namba, *Jap. J. Appl. Phys.* **24** L705 (1985).
13. S. Thomas III, K. K. Ko and S. W. Pang, *J. Vac. Sci. Technol. A* **13** 894 (1995).
14. C. R. Eddy, Jr., O. Glembocki, D. Leonhardt, V. A. Shamanian, R. T. Holm, B. D. Thoms, J. E. Butler and S. W. Pang, *J. Electron. Mater.* **26** 1320 (1997).
15. D. Leonhardt, C. R. Eddy, Jr., V. A. Shamanian, R. T. Holm, O. J. Glembocki, B. D. Thomas, D. S. Katzer and J. E. Butler, *Jap. J. Appl. Phys.* **37** L577 (1998).
16. D. Leonhardt, C. R. Eddy, Jr., V. A. Shamanian, R. T. Holm, D. J. Glembocki and J. E. Butler, *J. Vac. Sci. Technol. A* **16** 1547 (1998).
17. C. R. Eddy, Jr., D. Leonhardt, S. R. Douglass, B. D. Thoms, V. A. Shamanian and J. E. Butler, *J. Vac. Sci. Technol. A* **17** 38 (1999).
18. J. Canteloup, J-Cl. Common, *Colloque International sur des Procédés Plasma*, 1993
19. Jerry Stefani, Stephanie Watts Butler, *J. Electrochemical Society*, 141, No.5, 1995
20. B. Drevillon, *Progress in Crystal Growth and Characterisation of Materials* 27, No1
21. Gabriel G. Barna, 'Dry Etch Processes and Sensors' *Solid State Technology*, Vol. 37, No 1, 1994
22. Z. Knittl, *Optics of Thin Films*, J. Wiley & Sons, 1976

1. ACKNOWLEDGMENTS

Technical support from Mr. L. Heckerd at PTI is greatly appreciated. The work at UF is partially supported by a DOD MURI, monitored by AFOSR (H. C. DeLong), contract no. F49620-96-1-0026.

Table 1 shows band gap energy and wavelength of prepared GaAs and $\text{Al}_x\text{Ga}_{1-x}\text{As}$ (i.e. $x = 0.3 \sim 0.92$).

	Band Gap energy at room temp. (eV)	Wavelength (nm)	refractive index ($\lambda = 905$ nm)	refractive index ($\lambda = 670$ nm)
GaAs	1.35	918	3.54	3.78
$\text{Al}_{0.27}\text{Ga}_{0.73}\text{As}$	1.57	790	3.36	3.55
$\text{Al}_{0.5}\text{Ga}_{0.5}\text{As}$	1.76	707	2.93	3.20
$\text{Al}_{0.92}\text{Ga}_{0.08}\text{As}$	2.10	592	2.64	2.70